

Phosphorus Donors in Highly Strained Silicon

Hans Huebl,* Andre R. Stegner, Martin Stutzmann, and Martin S. Brandt

Walter Schottky Institut, Technische Universität München, Am Coulombwall 3, 85748 Garching, Germany

Guenther Vogg and Frank Bensch

Fraunhofer Institut für Zuverlässigkeit und Mikrointegration IZM, Institutsteil München, Hansastrasse 27d, 80686 München, Germany

Eva Rauls

Institut for Fysik og Astronomi, Aarhus Universitet, Ny Munkegade, Bygning 1520, 8000 Aarhus C, Denmark

Uwe Gerstmann

Institut de Minéralogie et de Physique des Milieux Condensés, Université Pierre et Marie Curie, Campus Boucicaut, 140 rue de Lourmel, 75015 Paris, France

(Received 27 July 2006; published 18 October 2006)

The hyperfine interaction of phosphorus donors in fully strained Si thin films grown on virtual $\text{Si}_{1-x}\text{Ge}_x$ substrates with $x \leq 0.3$ is determined via electrically detected magnetic resonance. For highly strained epilayers, hyperfine interactions as low as 0.8 mT are observed, significantly below the limit predicted by valley repopulation. Within a Green's function approach, density functional theory shows that the additional reduction is caused by the volume increase of the unit cell and a relaxation of the Si ligands of the donor.

DOI: [10.1103/PhysRevLett.97.166402](https://doi.org/10.1103/PhysRevLett.97.166402)

PACS numbers: 71.55.Cn, 03.67.Lx, 76.30.-v, 83.85.St

At present, several approaches for solid state-based quantum computing hardware are actively pursued. The possible integration with existing microelectronics and the long decoherence times [1–3] are particular advantages of concepts [4–7] using the nuclear or electronic spins of phosphorus donors in group IV semiconductors as qubits. These concepts require gate-controlled exchange coupling between neighboring donors. However, to control the exchange coupling in semiconductors with an indirect band structure such as Si, the donor atoms have to be positioned with atomic precision [8] due to Kohn-Luttinger oscillations of the donor wave function [5,9,10]. Under uniaxial compressive strain in the [001] direction, two conduction band (CB) minima are lowered in energy, which leads to a suppression of the oscillatory behavior of the wave function for donors located in the (001) lattice plane [9]. The strain will also affect the wave function at the donor atom, which can be observed directly via the hyperfine (hf) interaction between the donor electron and its nucleus [9,11]. In this letter, we experimentally and theoretically study the hf interaction of phosphorus donors in silicon as a function of uniaxial compressive strain in thin layers of Si on virtual SiGe substrates, extending the regime investigated by Wilson and Feher [11] by a factor of 20 to higher strains. We find that the reduction of the hf interaction significantly exceeds the limit predicted so far [5,9,11]. By *ab initio* density functional theory (DFT) calculations using a Green's function approach [12], we are able to show that this reduction is caused by the strain-induced lattice distortion and a relaxation of the Si lattice next to the P atoms. As the nuclear exchange mediated by the overlap of the donor wave function scales with the square

of the hf interaction, these results have a direct impact on the rate at which two-qubit operations can be performed [4].

The strained P-doped Si epilayers studied with $[\text{P}] \approx 1 \times 10^{17} \text{ cm}^{-3}$ were grown by chemical vapor deposition lattice matched on virtual relaxed $\text{Si}_{1-x}\text{Ge}_x$ substrates optimized for low dislocation densities [13]. These intrinsic virtual substrates consist of a 0.3 μm Si buffer on 30 Ωcm Si:B (001), a variable sequence of $\text{Si}_{1-y}\text{Ge}_y$ buffer layers with stepwise increasing y , and a final 2 μm $\text{Si}_{1-x}\text{Ge}_x$ buffer with $x = 0.07, 0.15, 0.20, 0.25,$ or 0.30. High-resolution x-ray diffraction (HRXRD) on the 004 and 224 reflexes was used to determine the lattice constants of the SiGe layers yielding the Ge content and degree of relaxation of the virtual substrate [14,15]. The $\text{Si}_{1-x}\text{Ge}_x$ layer determines the strain of the Si epilayer: The larger lattice constant of SiGe alloys compared to Si leads to biaxial tensile strain, accompanied by a compensating uniaxial compressive strain in growth direction (cf. inset of Fig. 1). All Si:P epilayers have a thickness of 15 nm, well below the critical thickness of Si on $\text{Si}_{0.7}\text{Ge}_{0.3}$ [16].

Figure 1 shows the 224 HRXRD reciprocal space map for the $\text{Si}_{0.7}\text{Ge}_{0.3}$ sample. The peak arising from the Si wafer is set to match the lattice constant of Si (5.4310 Å) [17]. Extending to lower reciprocal lattice units $q_{\parallel} = \sqrt{2}\lambda/a_{\parallel}$ (in plane) and $q_{\perp} = \sqrt{4}\lambda/a_{\perp}$ (out of plane), a set of diffraction peaks from the SiGe buffer layers is observed, followed by the peak of the virtual substrate. The slight deviation from the values expected for fully relaxed $\text{Si}_{1-x}\text{Ge}_x$ (black solid line, [14]) indicates a degree of relaxation of 96.4% of the virtual substrate. Additionally, Fig. 1 shows at $q_{\perp} = 0.5715$ ($a_{\perp} = 5.3912 \text{ Å}$) and $q_{\parallel} = 0.39686$

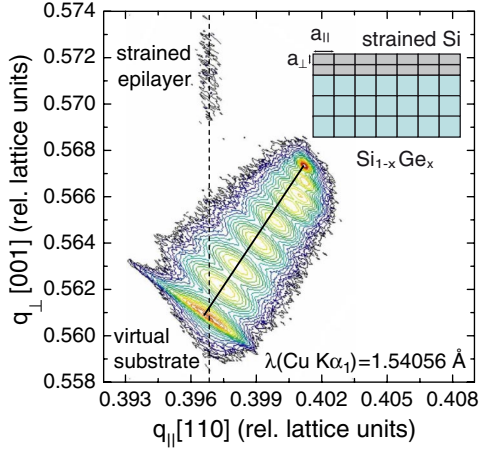


FIG. 1 (color online). HRXRD reciprocal space map of the 224 reflex of a 15 nm thick fully strained Si film on a $\text{Si}_{0.7}\text{Ge}_{0.3}$ virtual substrate (log-scaled isointensity plot). The straight line represents q_{\parallel} and q_{\perp} predicted for relaxed $\text{Si}_{1-x}\text{Ge}_x$ with $0 \leq x \leq 0.3$ [17].

($a_{\parallel} = 5.4898 \text{ \AA}$) the diffraction by the strained Si epilayer. The perfect agreement of q_{\parallel} of the Si epilayer and the virtual substrate reflects the fully strained pseudomorphic growth. Note that the compression in growth direction is in accordance with linear elasticity theory. With $C_{11} = 165.6 \text{ GPa}$ and $C_{12} = 63.9 \text{ GPa}$ as the stiffness constants of Si [15], the relation $\epsilon_{\perp} = -2C_{12}/C_{11}\epsilon_{\parallel}$ between in- and out-of-plane strains $\epsilon_{\parallel} = (a_{\parallel} - a_{\text{Si}})/a_{\text{Si}}$ and $\epsilon_{\perp} = (a_{\perp} - a_{\text{Si}})/a_{\text{Si}}$ predicts a value of $a_{\perp} = 5.3856 \text{ \AA}$ on the $\text{Si}_{0.7}\text{Ge}_{0.3}$ substrate, in reasonably good agreement with a_{\perp} obtained from Fig. 1, considering the width of the reflex from the Si layer caused by its thickness. Hence, the strain values for the different strained Si samples are obtained from the relaxed in-plane lattice constants of the corresponding SiGe buffers using linear elasticity theory.

To observe the small amount of P donors in the thin strained layer with high sensitivity, we use electrically detected magnetic resonance (EDMR), which monitors spin resonance via the influence of spin selection rules on charge transport processes [18–20]. The EDMR experiments were performed in a dielectric ring microwave resonator using a HP83640A microwave source and measuring the spin-dependent photoconductivity at $T = 5 \text{ K}$ in a liquid He flow cryostat under illumination with white light from a tungsten lamp. Resonant changes $\Delta I/I \approx 10^{-5}$ of the photocurrent I were detected using a current amplifier, lock-in detection, and magnetic field modulation with 0.2 mT at 1.124 kHz. All spectra were obtained using a microwave power of 50 mW and are normalized to a microwave frequency of 9.749 GHz.

Figure 2 shows the EDMR signal observed as a function of the applied magnetic field for different angles between the [001] direction of the Si epilayer and the externally applied magnetic field \vec{B}_0 . In the range of $B_0 = 346.5$ to 348 mT, anisotropic lines due to the P_{b0} center at the

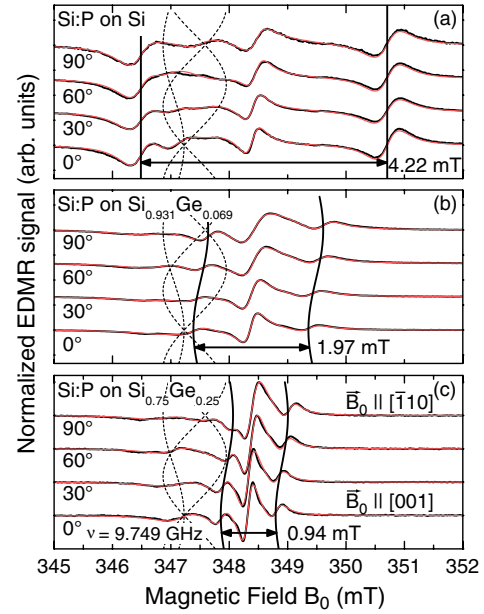


FIG. 2 (color online). Electrically detected magnetic resonance of P donors in relaxed and fully strained Si epilayers on three different $\text{Si}_{1-x}\text{Ge}_x$ virtual substrates as a function of the orientation of the [001] growth direction with respect to the magnetic field \vec{B}_0 for a rotation around [110]. To extract spectroscopic information, the spectra have been fitted using Lorentzian lines. The sum of these lines is shown in red (light gray). The dotted lines represent the resonances of P_{b0} centers at the Si/SiO_2 interface.

Si/SiO_2 interface are observed with their characteristic anisotropy [21,22] (dashed lines in Fig. 2). Within the resolution of our experiment, these resonances remain unchanged in the strained layers. The dominant central line with $g = 1.9994$ in the unstrained sample becomes slightly anisotropic under strain and could be assigned to CB electrons [23]. In the unstrained Si layer [cf. Fig. 2(a)], also the characteristic two hf-split lines of P in Si with a separation of $A_{\text{hf}} = 4.2 \text{ mT}$ are easily resolved. The hf lines are isotropic as indicated by the black vertical lines with a center of gravity at $g = 1.9985$, well known for unstrained c -Si [23,24].

In contrast, the hf-split resonances become anisotropic in strained epilayers as indicated by the black lines in Fig. 2(b) and 2(c). For Si on $\text{Si}_{0.93}\text{Ge}_{0.07}$ ($\epsilon_{\perp} = -0.00199$), they can be described with an isotropic hf interaction of 1.97 mT and an anisotropic g factor which varies by $\Delta g = (1.46 \pm 0.1) \times 10^{-3}$ from $\vec{B}_0 \parallel [1\bar{1}0]$ to $\vec{B}_0 \parallel [001]$. Figure 2(c) shows the results for the epilayer with $\epsilon_{\perp} = -0.00729$ on $\text{Si}_{0.75}\text{Ge}_{0.25}$. Here, the isotropic hf splitting decreases to 0.94 mT, while $\Delta g = (1.21 \pm 0.06) \times 10^{-3}$. The small hf splittings exclude significant segregation of P into the SiGe layers during the growth, which would lead to larger splittings [25,26].

For an isolated P donor atom in unstrained Si, the isotropic Fermi-contact hf interaction A_{hf} is given by $8/3\mu_B\pi|\psi(0)|^2$ [11,27], where μ_B is Bohr's magneton

and $|\psi(0)|^2$ is the probability amplitude of the unpaired electron wave function at the nucleus, giving rise to the doublet of hf lines separated by $A_{\text{hf}} = 4.2$ mT in Fig. 2(a). To determine $|\psi(0)|^2$, we first note that the cubic crystal field leads to the formation of a singlet ground state plus a doublet and a triplet of excited states. Only the fully symmetric singlet ground state has a nonvanishing probability amplitude at the nucleus, so that ψ can be written as a superposition $\psi = \sum_{i=1}^6 (1/\sqrt{6})\Phi_i$ of the six valleys contributing to the donor. Here, each Φ_i is a product of the corresponding CB Bloch wave function and a hydrogenic envelope function. The probability of the unpaired electron at the nucleus $|\psi(0)|^2$ becomes $(1/6)|\sum_{j=1}^6 \Phi_j(0)|^2 = 6|\Phi(0)|^2$, since due to symmetry $\Phi_i(0) = \Phi(0)$ for all i . Assuming that the only effect of strain is the change of relative population of the CB minima, we similarly find $\psi = \sum_{i=1}^2 (1/\sqrt{2})\Phi_i$ and $|\psi(0)|^2 = 2|\Phi(0)|^2$ under high uniaxial strain, when only two CB minima contribute. Therefore, in the fully strained case, the hf interaction should be $1/3$ of A_{hf} in the unstrained case. In contrast, in Fig. 2 we already observe a reduction to $0.21A_{\text{hf}}$. Based on group and linear elasticity theory, Wilson and Feher [11] have evaluated the analytical dependence of $A_{\text{hf}}(\chi)$ on the so-called valley strain $\chi = -\frac{\Xi_u}{3\Delta_c} (1 + \frac{2C_{12}}{C_{11}})\epsilon_{\parallel}$, where $\Xi_u = 8.6$ eV [28] is the uniaxial deformation potential, and $6\Delta_c = 2.16$ meV [29] is the energy splitting of the singlet and doublet state in the unstrained material. In Fig. 3, a comparison of the prediction of Eq. (2) in Ref. [11] (dashed line) with the hf splittings determined experimentally (solid circles) clearly shows that pure valley repopulation is not able to describe the experimental data for $x > 0.07$. An empirical treatment of additional radial redistribution effects predicts only $0.30A_{\text{hf}}$ for $\chi = -89$ ($x = 1$) [30]. Regarding quantum logic applications, the reduction in the hf interaction from $0.33A_{\text{hf}}$ to $0.21A_{\text{hf}}$ observed here reduces the maximum rate of an exchange mediated SWAP operation between two ^{31}P nuclear magnetic moments to $(0.21/0.33)^2 \approx 40\%$.

An *ab initio* calculation of hf interactions is demanding, but necessary to clarify the situation. Already for the unstrained case, the delocalization of the donor wave function leads to problems in describing the magnetization distribution correctly [31]. Whereas the energetic position of shallow levels as well as the geometries obtained by usual supercell calculations can be expected to be in accordance with experimental data, the hf interactions are generally overestimated [12,32]. Recently, a Green's function approach (using a linear muffin-tin orbital basis set, LMTO-GF) has been shown to circumvent this problem [12]. By analyzing the donor-induced resonance at the bottom of the CB, it becomes possible to describe the central-cell correction to effective mass theory by first principles with an accuracy that allows a prediction of superhyperfine interactions for shallow donor states including the Kohn-Luttinger oscillations [12,33].

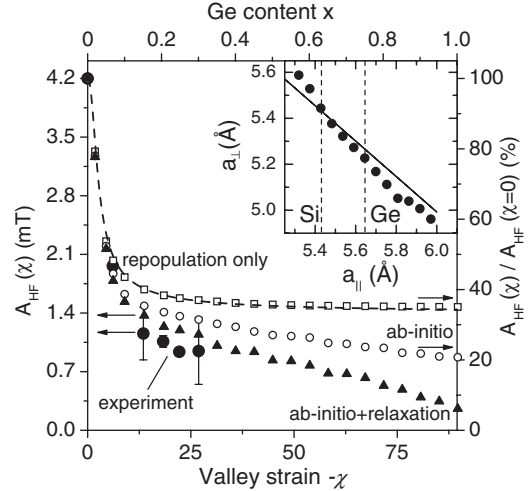


FIG. 3. Hyperfine splittings observed for P in fully strained Si epilayers on $\text{Si}_{1-x}\text{Ge}_x$ substrates as a function of x and the resulting valley strain. The black dots indicate the experimental data. The dashed line represents the behavior expected by valley repopulation [11]. The DFT results for valley repopulation only are indicated by open squares, the results including the strain-induced change in the volume of the unit cell by open circles, and those additionally including relaxation of the P nearest neighbors by solid triangles. For the latter and the experimental data the absolute values A_{hf} are shown; the remaining data refer to the relative scale. The inset shows the out-of-plane lattice constant a_{\perp} of thin Si layers (thickness 12 unit cells) as a function of the in-plane lattice constant a_{\parallel} predicted by SCC-DFTB compared to linear elasticity theory indicated by the straight line. Pseudomorphic Si layers on pure Si and Ge substrates are shown by dashed lines.

In the case of a strained host material, excited states are admixed to the former pure singlet ground state. An application of DFT is only possible in combination with linear elasticity theory: Because of the applied strain, the symmetry of the P donor is reduced, and the resonance at the bottom of the CB, transforming according to the a_1 representation in the unstrained case, now shows admixtures of the b_1 and b_2 representations of D_{2d} symmetry. The location of the P donor atom in their nodal planes implies a correlation of these b_1 - and b_2 -like orbitals with the admixed doublet state. Since, furthermore, only one component of the diamagnetic doublet state contributes to the singlet ground state under strain [11], it is reasonable to construct the spin densities, which enter the self-consistent DFT total energy calculations for a given valley strain, by $n^{\sigma}(r) = [1 - \alpha(\chi)]n_{a_1}^{\sigma}(r) + \alpha(\chi)n_{b_1}^{\sigma}(r)$, where $\sigma = |\uparrow\rangle$ or $|\downarrow\rangle$. Here, $\alpha(\chi)$ is obtained from the strain-dependent admixture of the doublet states determined by linear elasticity theory [see Eq. (C6) in Ref. [11]]. Figure 3 shows that the spin densities constructed this way allow a reasonable description of the pure valley repopulation effect, since for an unrelaxed structure of an ideal Si crystal, the results obtained by Wilson and Feher [11] are nicely reproduced after the self-consistent cycle (cf. open squares in Fig. 3).

We are now able to take into account explicitly *by first principles* the strain of the Si lattice as well as the relaxation around the P donors within. For the optimization of the strained Si cells, we used the self-consistent charge DFT-based tight binding (SCC-DFTB) approach [34]. Optimization of long slabs (up to 12 unit cells along the [001] direction) shows an almost linear dependence of the compression along [001] as an answer to the tensile strain in the (001) plane (cf. inset of Fig. 3). This result confirms that linear elasticity theory remains valid in the complete regime investigated, even up to $x = 1$. The hf parameters calculated with LMTO-GF under these assumptions (cf. open circles in Fig. 3) already become smaller since the donor wave function becomes more delocalized as a result of the enhanced volume.

This tendency is enhanced, if local relaxation around the P donors is taken into account: According to SCC-DFTB calculations on large, explicitly strained supercells with 512 atoms, this relaxation is dominated by a slight reduction of the bond-length between the P donor and its nearest Si ligands by about 1%, nearly independent of the strength of the tensile strain in the plane of the Si epilayer and already present in the unstrained case. Recalculating $A_{\text{hf}}(\chi)$ for this geometry, we find a further reduction (solid triangles in Fig. 3). While the predicted absolute value A_{hf} is ≈ 2 mT too large in the unstrained case without nearest neighbor relaxation, A_{hf} is now in good accordance with the experiment for all χ . The hf interaction observed can thus be explained by the increased volume of the unit cell together with a slight inward relaxation of the nearest Si neighbors. Since already such a small relaxation hugely influences the predicted relative hf splittings, the remaining discrepancy between experiment and theory can be attributed to uncertainties due to the flatness of the total energy surface in Si [35]. According to our DFT calculation, the decrease of the central P-related hf interaction is accompanied by an increase of the superhyperfine interaction with neighboring ^{29}Si atoms which could be verified by electron-nuclear double resonance (ENDOR) or electrically detected ENDOR [19].

Finally, the anisotropy of the g factor observed here is somewhat larger than previously reported [11,36]. Note that a single-valley effect arising from an admixture of the doublet is not expected for uniaxial strain in [001] direction, dominant in our samples. Rather, a pure repopulation effect is expected [11,37,38]. Thus, a detailed calculation of the g factor under strain including local relaxation is warranted.

This work was supported by the Deutsche Forschungsgemeinschaft (SFB 631 and Ge 1260/3-1).

*Corresponding author.

Electronic address: huebl@wsi.tum.de

[1] J.T.G. Castner, Phys. Rev. Lett. **8**, 13 (1962).

- [2] A.M. Tyryshkin, S.A. Lyon, A.V. Astashkin, and A.M. Raitisimring, Phys. Rev. B **68**, 193207 (2003).
- [3] J.P. Gordon and K.D. Bowers, Phys. Rev. Lett. **1**, 368 (1958).
- [4] B.E. Kane, Nature (London) **393**, 133 (1998).
- [5] B.E. Kane, Fortschr. Phys. **48**, 1023 (2000).
- [6] R. Vrijen *et al.*, Phys. Rev. A **62**, 012306 (2000).
- [7] L.C.L. Hollenberg *et al.*, Phys. Rev. B **69**, 113301 (2004).
- [8] S.R. Schofield, N.J. Curson, M.Y. Simmons, F.J. Rueß, T. Hallam, L. Oberbeck, and R.G. Clark, Phys. Rev. Lett. **91**, 136104 (2003).
- [9] B. Koiller, X. Hu, and S. Das Sarma, Phys. Rev. B **66**, 115201 (2002).
- [10] C.J. Wellard *et al.*, Phys. Rev. B **68**, 195209 (2003).
- [11] D.K. Wilson and G. Feher, Phys. Rev. **124**, 1068 (1961).
- [12] H. Overhof and U. Gerstmann, Phys. Rev. Lett. **92**, 087602 (2004).
- [13] S. Kreuzer, F. Bensch, R. Merkel, and G. Vogg, Mater. Sci. Semicond. Process. **8**, 143 (2005).
- [14] J.P. Dismukes, L. Ekstrom, and R.J. Paff, J. Phys. Chem. **68**, 3021 (1964).
- [15] N.S. Orlova, Cryst. Res. Technol. **24**, K39 (1989).
- [16] S.B. Samavedam *et al.*, J. Vac. Sci. Technol. B **17**, 1424 (1999).
- [17] P. Becker, P. Seyfried, and H. Siegert, Z. Phys. B **48**, 17 (1982).
- [18] J. Schmidt and I. Solomon, Comptes Rendu **263**, 169 (1966).
- [19] B. Stich, S. Greulich-Weber, and J.-M. Spaeth, Appl. Phys. Lett. **68**, 1102 (1996).
- [20] M.S. Brandt, S.T.B. Goennenwein, T. Graf, H. Huebl, S. Lauterbach, and M. Stutzmann, Phys. Status Solidi (c) **1**, 2056 (2004).
- [21] E.H. Poindexter, P.J. Caplan, B.E. Deal, and R.R. Razouk, J. Appl. Phys. **52**, 879 (1981).
- [22] A. Stesmans and V.V. Afanas'ev, J. Appl. Phys. **83**, 2449 (1998).
- [23] C.F. Young, E.H. Poindexter, G.J. Gerardi, W.L. Warren, and D.J. Keeble, Phys. Rev. B **55**, 16245 (1997).
- [24] P.R. Cullis and J.R. Marko, Phys. Rev. B **11**, 4184 (1975).
- [25] H. Volmer and D. Geist, Phys. Status Solidi **62**, 367 (1974).
- [26] M. Höhne, U. Juda, J. Wollweber, D. Schultz, J. Donecker, and A. Gerhardt, Mater. Sci. Forum **196–201**, 359 (1995).
- [27] W. Kohn, Solid State Phys. **5**, 257 (1957).
- [28] V.J. Tekippe, H.R. Chandrasekhar, P. Fisher, and A.K. Ramdas, Phys. Rev. B **6**, 2348 (1972).
- [29] A.K. Ramdas and S. Rodriguez, Rep. Prog. Phys. **44**, 1297 (1981).
- [30] H. Fritzsche, Phys. Rev. **125**, 1560 (1962).
- [31] E. Hale and R. Mieher, Phys. Rev. **184**, 739 (1969).
- [32] E. Rauls, M.V.B. Pinheiro, S. Greulich-Weber, and U. Gerstmann, Phys. Rev. B **70**, 085202 (2004).
- [33] W. Kohn and J. Luttinger, Phys. Rev. **98**, 915 (1955).
- [34] T. Frauenheim, G. Seifert, M. Elstner, Z. Hajnal, G.J.D. Porezag, S. Suhai, and R. Scholz, Phys. Status Solidi (b) **217**, 41 (2000).
- [35] U. Gerstmann, E. Rauls, H. Overhof, and T. Frauenheim, Phys. Rev. B **65**, 195201 (2002).
- [36] C.F.O. Graeff, M.S. Brandt, M. Stutzmann, M. Holzmann, G. Abstreiter, and F. Schäffler, Phys. Rev. B **59**, 13242 (1999).
- [37] L.M. Roth, Phys. Rev. **118**, 1534 (1960).
- [38] L. Liu, Phys. Rev. Lett. **6**, 683 (1961).